Accurate Determination of Skin Flux from Flow-Through Diffusion Cell Data

Daniel J. Harrison[1] and Kristine Knutson[1,2]

Received April 19, 1995; accepted August 21, 1995

Purpose. The goal of this investigation was to demonstrate whether the intrinsic flux of a drug diffusing across a membrane mounted in a flow-through diffusion cell may be accurately and easily determined by accounting for the accumulation in the receiver chamber.
Methods. Mathematical modeling, applied to transdermal diffusion, was used to calculate receiver concentration data for single layer and bilayer membranes. The data were interpreted using two apparent flux values, J_{app1} and J_{app2}. J_{app1} has been used extensively in the literature, but did not account for accumulation in the receiver. J_{app2} did take the accumulation into consideration.
Results. The results confirm that, generally, J_{app1} values were not accurate estimates of the intrinsic flux. J_{app2} values were significantly more accurate, especially prior to the maximum in receiver concentration.
Conclusions. J_{app2} was an accurate measurement of intrinsic flux over the entire experimental time period, except at time zero. It was more accurate because it accounted for solute accumulation in the receiver compartment. The accuracy of the J_{app2} approximation was practically independent of receiver volume, flow rate and donor volume. For very slowly permeating drugs, or a very small receiver volume combined with a high flow rate, the J_{app1} estimate accurately reflected the intrinsic flux. Early time data were required to properly account for accumulation in the receiver cell. If such data were not available, the inverse Laplace method of determining intrinsic flux was preferable to the J_{app2} calculation.

KEY WORDS: flow-through diffusion cell; apparent flux; intrinsic flux; transdermal.

INTRODUCTION

Flow-through type diffusion cells have been used to measure drug flux across skin and other membranes of interest. These cells have the advantage that the experimental apparatus may be automated, allowing for a rapid accumulation of diffusion data. In a typical system, the permeant dissolved in the donor solution was added to the donor cell to initiate the experiment. The drug diffused across the skin and entered the receiver chamber. With proper mixing, the receiver behaved as a well mixed vessel and therefore the concentration of the drug entering the outflow tubing was the same as the concentration in the receiver chamber. In an automated system, the tubing transferred the liquid to a sampling vial or test tube for a specified time interval (the sampling interval). A good analysis of the flow-through receiver cell has been given by Sclafani et al. 1993 (1).

Flow-through diffusion cells have been extensively used to measure skin flux *in vitro* (2-15). Many of these studies used automated systems for data collection. The drugs that were tested varied substantially in molecular weight and in physical properties, from highly lipophilic to very hydrophilic. All of the studies used the J_{app1} approximation to estimate drug flux, regardless of the magnitude of the flux. None of the studies derived the apparent flux equation.

The objective of the transdermal permeation experiment has been to determine the drug flux through the skin, but the experiment provided receiver cell concentration data as a function of time. Consequently, some authors did not determine flux values from their permeation data. Cooper (2) presented his results strictly in terms of cumulative amount entering the sample vials versus time. Knepp et al. (3) and Kai et al. (4) did not determine the flux of drug, but instead reported a release rate in terms of (%dose/hr). This was estimated from the total amount of drug collected over each sampling interval. Addicks et al. (5) estimated an apparent steady-state permeability coefficient from regression analysis of the cumulative amount permeated versus time. They found that the permeability coefficients calculated from flow-through cell data compared well with those determined using a non-flow Franz-type cell, where the entire receiver volume was replaced each time a sample was taken. In a subsequent investigation, Addicks and coworkers (6) compared the fractional dose permeated to predicted values, without determining drug flux.

Reifenrath and colleagues (7) compared skin penetration using three types of diffusion cells: a flow-through cell with a low volume receiver (0.3 ml), a second flow-through cell with a high receiver volume (4.3 ml) and a static Franz-type cell with the largest receiver volume (7.5 ml). Using benzoic acid and estradiol, these investigators found that the output from the low volume flow-through cell tracked the flux from the static cell, but that the output from the high volume cell lagged behind the other output values. When the accumulation of drug within the high volume cell was taken into account, however, the flux values agreed quite well with the fluxes from the other cells. Bronaugh and Stewart (8) also reported good agreement between drug fluxes measured in a low volume flow-through cell and those measured in a static diffusion cell.

Since the flux must be calculated from the concentration versus time data, proper analysis of the flow-through diffusion cell is critically important in the accuracy of the calcu-

[1] Department of Pharmaceutics and Pharmaceutical Chemistry, University of Utah, Salt Lake City, Utah 84112.
[2] To whom correspondence should be addressed.

Notation: A, diffusion area; C_i, concentration in membrane layer i; C_{don}, donor cell concentration; C_{dono}, initial donor concentration; C_{rec}, receiver cell concentration; C_{reci}, average receiver concentration over time interval i; D_{ei}, effective diffusivity of membrane layer i; F_{rec}, volumetric flow rate through receiver cell; h, thickness of first layer, stratum corneum; h_2, thickness of second layer, viable skin; H, total membrane thickness; J, drug flux; J_{app1}, first apparent drug flux, Equation 2; J_{app1i}, average apparent flux over time interval i; J_{app2}, second apparent drug flux, Equation 4; J_{intrin}, intrinsic drug flux; J_{max}, maximum flux of drug; K_i, partition coefficient, membrane layer i; k_p, permeability coefficient; m, number of node points in second layer; n, number of C_{rec} data points; t, time; t_{jmax}, time of maximum flux; V_{don}, donor cell volume; V_{rec}, receiver chamber volume; x, spatial coordinate; ΔQ_i, total amount sampled over time interval i; Δt, sampling duration for time interval.

lation. The general mass balance on the receiver chamber of a flow-through diffusion cell is:

$$V_{rec}\frac{dC_{rec}}{dt} = J\,A - F_{rec}C_{rec} \quad (1)$$

where V_{rec} is the volume of the receiver chamber, C_{rec} the receiver concentration, J the flux of drug out of the skin into the receiver compartment, A the area of skin available for diffusion and F_{rec} the liquid flow rate through the receiver chamber. The term (dC_{rec}/dt) is the accumulation of drug in the receiver cell. This mass balance assumes that the receiver is well mixed and that the incoming flow is drug free.

In order to simplify the mass balance, it is often assumed that the accumulation in the receiver chamber is so small that it is negligible. Initially this assumption seems reasonable, since the flow of liquid through the receiver chamber removes the drug, physically limiting accumulation. In this case the equation becomes:

$$J_{app\,1} = \frac{F_{rec}C_{rec}}{A} \quad (2)$$

The apparent flux calculated from Equation 2 is designated as J_{app1}, which is the same as J_{app} in the Sclafani et al. paper (1). Equation 2 is typically employed to estimate the average flux over each sampling interval (i) by utilizing the average (i.e. experimentally measured) receiver concentration (C_{reci}) for that interval. J_{app1i} is directly related to the total amount leaving the cell in that time period (ΔQ_i):

$$J_{app1i} = \frac{F_{rec}C_{reci}}{A} = \frac{1}{A}\frac{\Delta Q_i}{\Delta t} \quad (3)$$

Equation 3 has often been used to estimate the flux out of the skin from the experimental receiver concentration values. Akhter and coworkers (9), Goodman and Barry (10) and Williams and Barry (11) have used the same experimental setup for studying skin permeation. Akhter et al. (9) and Williams and Barry (11) estimated transdermal flux from the apparent steady-state values of cumulative amount penetrated versus time. Goodman and Barry (10) used Equation 3 to evaluate the flux since their results did not show a steady-state. Friend and colleagues (12) presented graphs of drug flux versus time, but did not specify how the flux was determined. Later, Friend et al. (13) and Catz and Friend (14) calculated the apparent simultaneous fluxes of drug and enhancer components using Equation 3.

Accounting for accumulation in the mass balance equation is a more general approach to the problem of determining the flux. When the accumulation term is included, Equation 1 may be rearranged to give a second apparent flux (J_{app2}):

$$J_{app2} = \frac{V_{rec}\frac{dC_{rec}}{dt} + F_{rec}C_{rec}}{A} \quad (4)$$

in the case of no flow, Equation 4 reduces to:

$$J_{app2} = \frac{V_{rec}}{A}\frac{dC_{rec}}{dt} \quad (5)$$

which has been used in the literature to analyze transdermal flux data from side-by-side diffusion cells without flow through the receiver chamber (16-18).

The principal goal of this investigation was to demonstrate that J_{app2} more accurately estimated the intrinsic flux out of the skin (J_{intrin}) than J_{app1} from the same set of receiver concentration data, as well as that J_{app2} may be efficiently and simply determined.

Sclafani and his colleagues (1) previously demonstrated that the apparent flux J_{app1} gives an inaccurate estimate of the intrinsic flux maximum, J_{max}, as well as the time of that maximum, t_{jmax}. It was shown that the intrinsic flux could be obtained by a numerical Laplace inversion of the apparent flux divided by a transfer function. They demonstrated their method using experimental data for ethanol diffusing across human skin. A second goal of this investigation was to show that in the all-too-common case of sparse data, the inverse Laplace approach yielded a more accurate intrinsic flux than did J_{app2}.

A numerical model of diffusion through a single or bilayer membrane was used to generate receiver cell concentration data under the same conditions presented by Sclafani et al. (1). From the receiver cell concentration data, the diffusion area, the receiver flow rate and the volume of the receiver chamber, J_{app1} and J_{app2} values were calculated. The intrinsic flux of the skin was calculated directly from the concentration profile of the skin/receiver interface. Plots of the two apparent flux values and the intrinsic flux as a function of time were then compared for various experimental configurations.

METHODS

Theoretical Model Development

Diffusion Modeling

A transdermal diffusion model based on a bilayer membrane in a diffusion cell was used to calculate transient diffusion data. Each layer was treated as homogeneous, where a constant effective diffusivity represented all transport pathways and an apparent partition coefficient represented the total uptake of the drug into all regions within each skin layer.

Transient diffusion was described by:

$$\frac{\partial C_i}{\partial t} = D_{ei}\frac{\partial^2 C_i}{\partial x^2} \quad (6)$$

where C_i represented the concentration of drug in layer i.

Two boundary conditions and one initial condition must be specified for each layer. Boundary conditions at the upper and lower surfaces were determined by partitioning from the donor and receiver cells, respectively:

$$\begin{aligned} &\text{at } x = 0, \quad C_1 = K_1 C_{don} \\ &\text{at } x = H, \quad C_2 = K_2 C_{rec} \end{aligned} \quad (7)$$

K_1 was the apparent partition coefficient of the first layer (stratum corneum) and K_2 the apparent partition coefficient of the second layer (viable epidermis-dermis).

No additional boundary conditions were needed for a

single layer membrane. For a bilayer membrane, however, two additional boundary conditions had to be specified. These conditions were specified at the boundary between the two layers, where the flux leaving the first layer (the stratum corneum) must be balanced by the flux entering the second (the viable epidermis-dermis) and a local equilibrium between the two layers was assumed to be:

$$\text{at } x = h, \qquad \frac{C_1}{C_2} = \frac{K_1}{K_2} \tag{8}$$

$$\text{and} \qquad D_{e1}\frac{dC_1}{dx} = D_{e2}\frac{dC_2}{dx}$$

Initial conditions were:

$$\text{at} \qquad t = 0, \qquad C_1 = C_2 = 0 \tag{9}$$

Mass balances on the donor and the receiver chambers completed the set of equations required. The mass balance on the donor cell was:

$$\frac{dC_{don}}{dt} = \frac{A}{V_{don}} D_{e1}\left.\frac{\partial C_1}{\partial x}\right|_{x=0} \tag{10}$$

And the mass balance on the receiver cell was expressed as:

$$\frac{dC_{rec}}{dt} = \frac{A}{V_{rec}} D_{e2}\left.\frac{\partial C_2}{\partial x}\right|_{x=H} - \frac{F_{rec}}{V_{rec}} C_{rec} \tag{11}$$

With initial conditions:

$$\text{at} \quad t = 0, \qquad C_{don} = C_{dono}, \qquad C_{rec} = 0 \tag{12}$$

The set of equations 6 - 12 constituted the bilayer diffusion model applied to an *in vitro* experimental arrangement. These equations were numerically solved using the method-of-lines (19), which reduced the partial differential equations to a set of ordinary differential equations (ODEs). This coupled set of ODEs was then solved using ODEPACK (20). A grid of 41 nodal points for each layer was adequate.

The intrinsic flux into the receiver chamber was determined from:

$$J_{intrin} = - D_{e2}\left.\frac{\partial C_2}{\partial x}\right|_{x=H} \tag{13}$$

Numerically, the concentration gradient at the skin/receiver chamber boundary was calculated with a second order equation:

$$\left.\frac{\partial C_2}{\partial x}\right|_{x=H} = \frac{C_{2,m-2} - 4\,C_{2,m-1} + 3\,C_{2,m}}{2\,\Delta x} \tag{14}$$

where m was the number of nodal points.

The model should generate receiver cell concentration and intrinsic flux data which agree with one's intuition about the physical realities of a flow-through cell with a finite donor. Initially the receiver concentration and the flux should be zero, but both should increase rapidly since the driving force for diffusion is greatest at the beginning of the experiment. There should be a short delay in the increase in receiver concentration until detectable quantities of drug have diffused across the skin membrane. However the receiver concentration cannot continue to increase indefinitely because the drug is being removed from the chamber in proportion to its concentration. In addition, the flux cannot continue to increase because of two factors: the donor cell is being depleted and the receiver cell concentration is increasing. Thus, both the receiver concentration and the flux should reach maximums and then decrease. The timing of the maximums is not necessarily the same. The flux should continue to drop as the donor cell is depleted. As the input to the receiver decreases, the receiver concentration should also further decrease. If the experiment is allowed to proceed to completion, the flux and the receiver concentration should fall to zero as the amount of drug in the donor is totally exhausted.

Analytical solutions to the transient diffusion equation (Equation 6) exist for simplified boundary conditions. Choi and Angello (21) assumed perfect source and sink conditions across a single layer membrane and used the analytical solution to obtain an expression for the drug flux leaving the skin in a flow-through cell. They then substituted that expression into the mass balance for the receiver cell (Equation 1) to obtain an equation for the receiver concentration as a

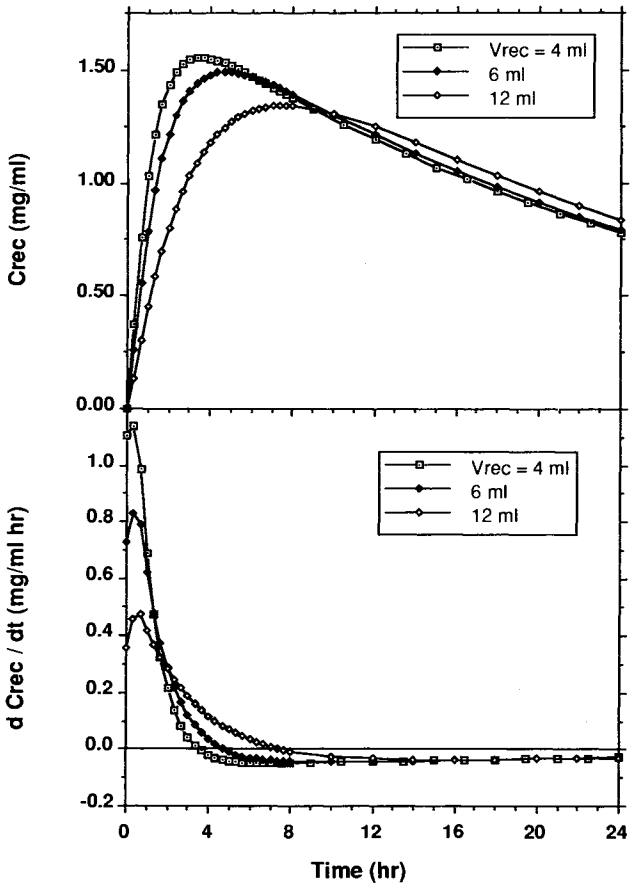

Fig. 1. Upper panel: Effect of receiver volume on calculated receiver concentrations. Same conditions as Figure 3 in Sclafani et al. (1). F_{rec} = 4 ml/hr, V_{don} = 0.5 ml, A = 5 cm^2, C_{dono} = 395 mg/ml; single layer membrane with $D_e = 2.0 \times 10^{-9}$ cm^2/sec, K = 1, h = 20 μm. Lower panel: Effect of receiver volume on the accumulation term. Values calculated from C_{rec} versus time data presented in upper panel.

Table I. Tabulated Values of Donor and Receiver Concentration Versus Time for V_{don} = 0.5 ml, V_{rec} = 4 ml, A = 5 cm^2 and F_{rec} = 4 ml/hr as Shown in Figures 1 and 2[a]

Time (hr)	C_{don} (mg/ml)	C_{rec} (mg/ml)	dC_{rec}/dt (mg/ml hr)	J_{intrin} (mg/cm^2 hr)	J_{app1} (mg/cm^2 hr)	J_{app2} (mg/cm^2 hr)
0.00	395.00	0.00	1.10E + 00	0.000	0.000	0.883
0.33	387.73	0.37	1.14E + 00	1.391	0.299	1.211
0.67	383.14	0.76	9.84E − 01	1.380	0.608	1.395
1.00	378.61	1.03	6.88E − 01	1.363	0.824	1.374
1.33	374.14	1.22	4.75E − 01	1.347	0.975	1.355
1.67	369.72	1.35	3.23E − 01	1.330	1.078	1.336
2.00	365.35	1.43	2.14E − 01	1.314	1.147	1.318
2.33	361.04	1.49	1.37E − 01	1.299	1.192	1.301
2.67	356.78	1.52	8.17E − 02	1.283	1.220	1.285
3.00	352.57	1.54	4.23E − 02	1.268	1.235	1.269
3.33	348.41	1.55	1.43E − 02	1.253	1.242	1.254
3.67	344.30	1.55	−5.49E − 03	1.238	1.243	1.239
4.00	340.24	1.55	−1.95E − 02	1.223	1.239	1.224
4.33	336.23	1.54	−2.93E − 02	1.209	1.233	1.209
4.67	332.26	1.53	−3.62E − 02	1.195	1.224	1.195
5.00	328.34	1.52	−4.09E − 02	1.181	1.213	1.181
.	.	.	.	.	.	.
19.50	195.97	0.91	−3.25E − 02	0.705	0.731	0.704
21.00	185.78	0.87	−3.08E − 02	0.668	0.693	0.668
22.50	176.12	0.82	−2.92E − 02	0.633	0.657	0.633
24.00	166.96	0.78	−2.77E − 02	0.600	0.622	0.600

[a] C_{don} and C_{rec} were calculated from the model. The apparent fluxes were based on the C_{rec} values: J_{app1} were calculated from Equation 3 and J_{app2} from Equation 4. The accumulation term was determined from Equations 15–18. Intrinsic flux values were calculated from Equation 13.

function of time. The equation was valid if depletion of the donor is negligible and the receiver concentration is close to zero. Under these conditions, there would be no maximums in the receiver concentration or the flux. Rather, steady state values would be attained. The analytical solution presented by Choi and Angello (21) for the receiver concentration and flux as a function of time served as a limiting test case for the present numerical model. When the donor concentration was held constant, the numerical model calculations were in excellent agreement with the analytical solution.

In order to determine the intrinsic flux from experimental data using the equations from Choi and Angello, the membrane thickness and the effective diffusivity must be determined.

Apparent Flux Estimates

Given the effective diffusivities and the partition coefficients of the two layers, the model calculated the receiver cell concentration and intrinsic flux as a function of time. The apparent flux estimates J_{app1} and J_{app2} were determined from the receiver concentration values as follows: J_{app1} was calculated from the receiver concentrations directly using Equation 3, while J_{app2} required a value for the accumulation term (dCrec / dt). This was determined numerically from the C_{rec} versus time data. For all but the first and last C_{rec} values, the accumulation term was estimated by:

$$\frac{dC_{rec,i}}{dt} = \frac{C_{rec,i+1} - C_{rec,i-1}}{2\,\Delta t} \qquad (15)$$

for equal time intervals. If the intervals were unequal, then the following equation was used:

$$\frac{dC_{rec,i}}{dt} = \frac{1}{2}\left(\frac{C_{rec,i+1} - C_{rec,i}}{\Delta t_2} + \frac{C_{rec,i} - C_{rec,i-1}}{\Delta t_1}\right) \qquad (16)$$

The accumulation terms for the first (1) and last (n) time points were estimated by the following second order approximations:

$$\frac{dC_{rec,1}}{dt} = \frac{-3C_{rec,1} + 4C_{rec,2} - C_{rec,3}}{2\,\Delta t} \qquad (17)$$

$$\frac{dC_{rec,n}}{dt} = \frac{C_{rec,n-2} - 4C_{rec,n-1} + 3C_{rec,n}}{2\,\Delta t} \qquad (18)$$

Given the estimates of the accumulation term, J_{app2} was then calculated from Equation 4.

It has been previously shown how increasing the sampling duration decreases the apparent flux peak height and skews the peak to longer times (1). Therefore, all the calculations in this investigation assumed very short (instantaneous) sampling durations.

RESULTS AND DISCUSSION

Most of the results shown here are from single layer membrane calculations. This allowed replication of the conditions presented by Sclafani et al. (1). The receiver volumes employed in the calculations cover the upper range of commercially available flow-through cells, 0.3 - 12 ml (1). As

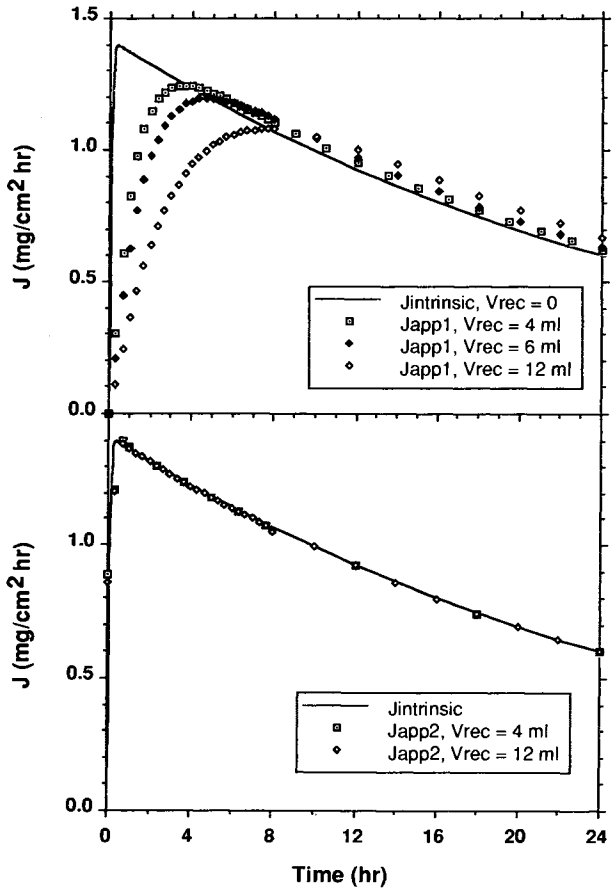

Fig. 2. Influence of receiver volume on apparent flux approximations to the intrinsic flux. The line represents the intrinsic flux and the discreet points the apparent flux values. F_{rec} = 4 ml/hr, V_{don} = 0.5 ml, A = 5 cm^2, C_{dono} = 395 mg/ml; single layer membrane with $D_e = 2.0 \times 10^{-9}$ cm^2/sec, K = 1, h = 20 μm. Upper panel: J_{appl} calculated from C_{rec} data in Figure 1. Lower panel: J_{app2} approximations based on the same data.

discussed below, this was the region where the J_{app2} analysis was the most appropriate.

Figure 1 presents a graph of the receiver concentration values as a function of receiver volume, calculated from the single layer model using the same conditions as Figure 3 in the Sclafani et al. paper. The C_{rec} curves in the two figures are virtually identical. Accumulation values (dC_{rec} / dt) were numerically calculated from the C_{rec} values using Equations 15-18 and are shown in the lower panel of Figure 1. For the V_{rec} equals 4 ml case, the values are tabulated in Table I. It is apparent that accumulation was highest during the earliest phase of the diffusion experiment, prior to the maximum in the C_{rec} curve. After the maximum, the accumulation term became negative and remained so for durations exceeding 24 hr. Thus, it may be anticipated that the assumption of negligible accumulation in the receiver was not valid at the earliest times and therefore that the J_{appl} estimate of intrinsic flux would be the least accurate prior to the maximum concentration. In addition, at the longer time periods when the accumulation term was negative, the J_{appl} estimate should be higher than the intrinsic flux.

Flux values, determined from the C_{rec} values in Figure 1, are presented in Figure 2, with the intrinsic flux plotted as a solid line and the apparent values plotted as discrete points. For the 4 ml case, Table I lists the apparent fluxes calculated from the C_{rec} values as well as the intrinsic flux. The J_{intrin} and J_{appl} curves are shown in the upper panel of Figure 2 and, as expected, are the same as in Figure 3 of Sclafani et al. (1). It is clear that the J_{appl} calculation substantially underestimated the early intrinsic flux, with highly erroneous J_{max} and t_{jmax} values. The size of this error decreased as the receiver chamber volume decreased. For very small receiver volumes, such as 0.4 ml (8), the J_{appl} and Ji_{ntrin} values were practically identical. The J_{appl} curve crossed the J_{intrin} curve at the maximum in the apparent flux. This was the point where the accumulation term equaled zero and the C_{rec} curve attained its maximum. Beyond this point, the apparent flux overestimated the intrinsic flux.

The lower panel of Figure 2 shows the J_{intrin} and J_{app2} curves. For the sake of clarity, only a limited number of points from the 4 and 12 ml calculations are plotted. In sharp contrast to the J_{appl} results, all of the J_{app2} values yielded highly accurate values of the intrinsic flux for all times except time zero. In addition, the J_{app2} accuracy did not depend on the receiver volume. In other words, highly accurate intrinsic flux values may be calculated even as the receiver volume becomes relatively large.

The increased accuracy of the apparent flux estimates when accounting for the accumulation of drug in the receiver compartment became apparent by further examination of Equation 4. The numerator in the equation is the sum of two terms, $V_{rec}\, dC_{rec}$ / dt and $C_{rec}\, F_{rec}$. Clearly, if $V_{rec}\, dC_{rec}$ / dt were much smaller than $C_{rec}\, F_{rec}$, then Equation 4 would reduce to Equation 3, the relationship for Jappl. Indeed, this would be the case when a very small receiver volume and a very high flow rate were used. However, assuming only that the accumulation term dC_{rec} / dt was small was not a sufficient reason to eliminate the ($V_{rec}\, dC_{rec}$ / dt) term. The relative contribution of the ($V_{rec}\, dC_{rec}$ / dt) term compared to the ($C_{rec}\, F_{rec}$) term was the important consideration. Since the experimental design not only minimized accumulation but also maintained receiver concentrations near zero (i.e. sink conditions), both the concentration and the accumulation were normally small. Therefore, the ($C_{rec}\, F_{rec}$) term and the ($V_{rec}\, dC_{rec}$ / dt) term may each significantly contribute to the flux.

The dimensionless ratio

$$\frac{\text{accumulation}}{\text{out}} = \frac{V_{rec}\dfrac{dC_{rec}}{dt}}{C_{rec}F_{rec}} \qquad (19)$$

is a measure of the relative contributions of the two terms. It was examined for conditions presented in Figure 1: a flow rate of 4 ml/hr and a receiver volume of 6 ml. At the maximum in accumulation (at 20 min), the ratio was 4.8. The ratio decreased with time, dropping to 0.5 by 100 min and to 0.05 around 225 min. Thus, the concentration term would not be expect to dominate the accumulation term until almost 4 hr after the experiment had begun.

The rate of accumulation in the receiver compartment is directly related to the permeability of the drug through the skin. Therefore, as the permeability decreased, the ratio ex-

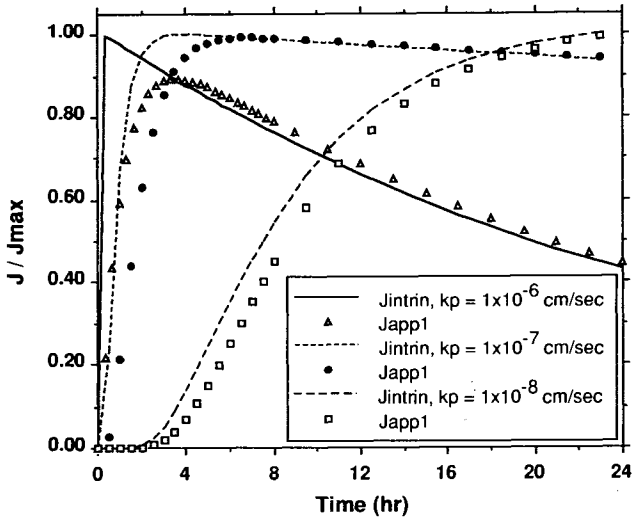

Fig. 3. Effect of drug permeability on the accuracy of the J_{appl} estimate. Solid and dashed lines are the intrinsic flux and the points are the J_{appl} values. Same conditions as those in Figure 2. Permeability decreased by reducing the effective diffusivity.

pressed in Equation 19 would be expected to decrease and the J_{appl} approximation would become more accurate. This was demonstrated in Figure 3, where a normalized flux is plotted for various permeabilities. The flux was normalized by the maximum flux for each case so that the curves may be plotted on the same scale. Again, the lines represent the intrinsic flux and the points represent the apparent flux, J_{appl}. Using the same conditions as Figure 2 and a receiver volume of 4 ml, the effective diffusivity was decreased twice by a factor of 10 to calculate the influence of a decreased permeability. It is apparent that as the drug permeability decreased from 1×10^{-6} to 1×10^{-8} cm/sec, the J_{appl} approximation increased in accuracy. In all three cases, however, the apparent flux continued to underestimate the true flux prior to the C_{rec} maximum.

The results from Figure 2 can be qualitatively compared with apparent flux data obtained by Goodman and Barry (10). In their control experiments, the drug flux attained a maximum very soon after diffusion was initiated and decreased for the duration of the experiment, the same type of behavior shown in Figure 2 for the intrinsic flux. Because Goodman and Barry used a very small receiver volume (0.0364 cm^3) and a relatively high flow rate, the mean residence time in the receiver cell was quite short, 1.1 min. Therefore, the J_{appl} approximation should be quite accurate under these conditions. Goodman and Barry theorized that the initial flux maximum was due to significant shunt diffusion through the skin. However, the mathematical model suggested that an early maximum may have actually been the result of depletion of the donor. In Goodman and Barry's investigation, the drug initially deposited on the uppermost skin layers may have been depleted.

As the number of early data points increased, the accuracy of the J_{app2} approximation also increased. The need for more early time data to increase accuracy did not necessarily require a greater total number of C_{rec} samples. The additional early time samples could be offset by fewer long term samples, which would not be needed to maintain J_{app2} accuracy. This could be accomplished by lengthening the sampling interval after the early time samples have been taken, usually after the first 3-4 hrs, depending on the permeability of the drug.

The effect of the receiver flow rate, F_{rec}, on flux is examined in Figure 4. For the same general conditions as Figure 2, the flow rate was varied from 0 to 4 ml/hr. The J_{intrin} and J_{appl} curves are shown in the upper panel for the same conditions as Figure 4 in Sclafani et al. (1). As the flow rate was reduced, the J_{max} and t_{jmax} values from J_{appl} became increasingly inaccurate. However, the J_{app2} values, presented in the lower panel, were excellent measures of the intrinsic flux, even as the flow rate was reduced to 1 ml/hr. The higher flow rate results fall on the intrinsic flux curve (data not shown).

Also included in the lower panel of Figure 4 are the results for zero flow through the receiver. Under such conditions, the expression for J_{app2} simplified to Equation 5 while the J_{appl} expression reduced to zero. As can be seen in this panel, the J_{app2} estimates under no flow conditions were slightly below the intrinsic flux values. However, the error in the J_{app2} estimate at zero flow is smaller than the error in the J_{appl} estimate at a flow rate of 4 ml/hr. Therefore, neither high flow rates nor a flow-through type diffusion cell would be required to obtain high accuracy in the measurements of

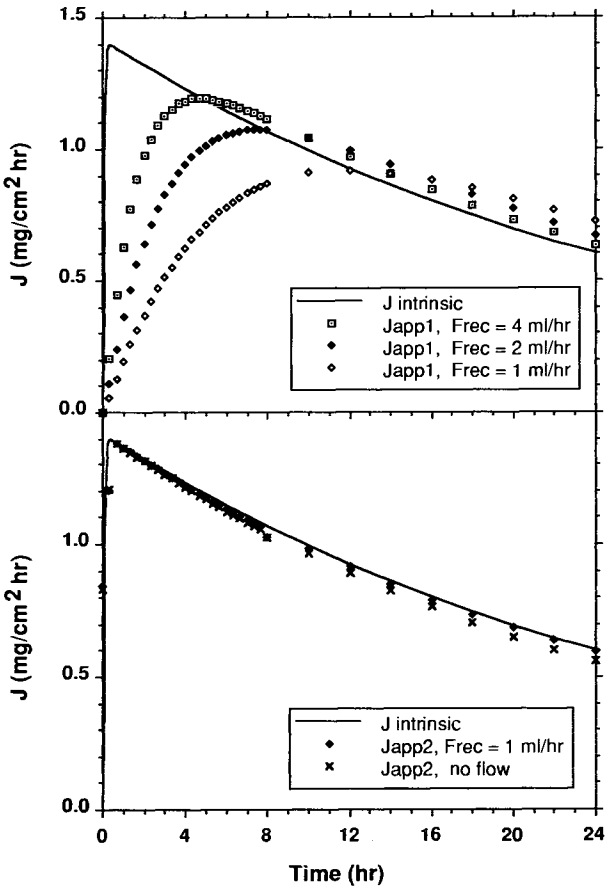

Fig. 4. Effect of receiver flow rate on apparent fluxes. V_{don} = 0.5 ml, V_{rec} = 6 ml. Transport properties same as those in Figure 2. Upper panel: J_{appl} approximations. Lower panel: J_{app2} approximations.

skin fluxes. However, a large number of C_{rec} samples would be required.

An important implication of that finding was that much higher concentrations in the sample vials could be tolerated. In other words, accurate flux values may be obtained even if strict sink conditions were not maintained during the experiment. This would be particularly desirable whenever increased C_{rec} values raised the accuracy of drug detection and concentration measurements. In addition, this would broaden the range of acceptable flow rates.

Figure 5 shows the influence of the donor volume on the apparent and intrinsic flux. In this figure, J_{intrin} curves were plotted as solid lines. In the upper panel, J_{app1} values were plotted as discrete points and it is obvious that the apparent J_{max} and t_{jmax} values were incorrect. The error in J_{max} increased and the error in t_{jmax} decreased as the donor volume decreased. In the lower panel, J_{app2} values again plotted as points produced accurate estimates of the intrinsic flux, except at zero time.

Based on the results in Figures 2, 4 and 5, the accuracy of the J_{app2} approximation was practically independent of the receiver volume, receiver flow rate and donor volume.

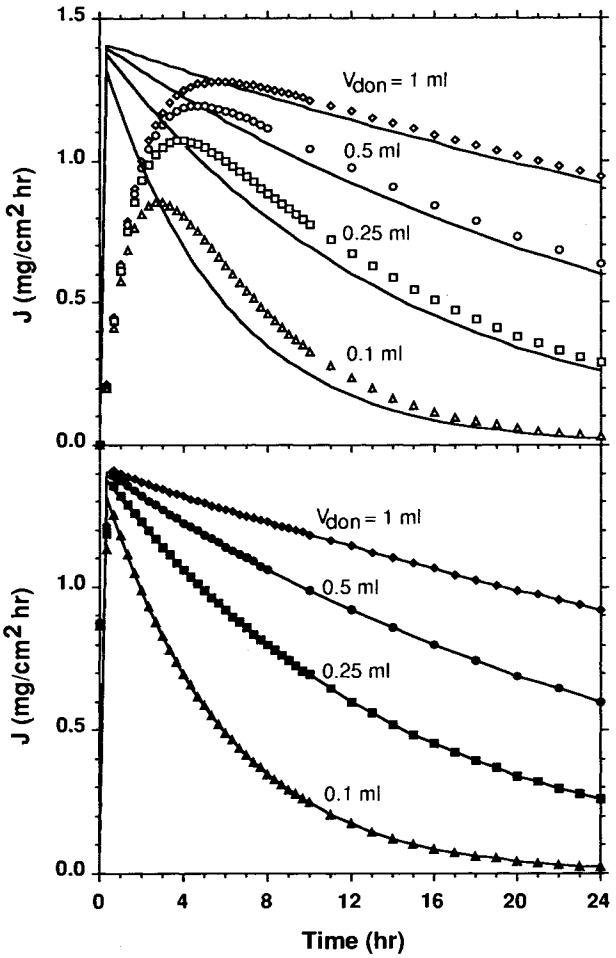

Fig. 5. Effect of donor volume on apparent and intrinsic fluxes. Same conditions as Figure 2 with V_{rec} = 6 ml, F_{rec} = 4 ml/hr. Lines represent the intrinsic fluxes and the discrete points represent the apparent fluxes. Upper panel: J_{app1} values. Lower panel: J_{app2} approximations. V_{don} values as listed.

Table II shows apparent and intrinsic flux data taken from Sclafani et al. (1) for ethanol diffusing through human skin. Using the stated values of diffusion area (5.0 cm^2) and receiver flow rate (4.74 ml/hr), the receiver concentrations were back calculated from the given flux data. From these concentrations and the receiver volume (6.5 ml), J_{app2} values were estimated from Equation 4 and are listed in the table. The accumulation term was numerically determined utilizing Equations 15-18. The maximum intrinsic flux Sclafani et al. (1) determined was 1.47 mg/cm^2 hr.

Comparison of the apparent flux values with the intrinsic flux in Table II revealed that both the J_{max} and the t_{jmax} values estimated from J_{app2} are more accurate than those based on J_{app1}. The J_{app2} calculation gave a good estimate of the intrinsic flux from the first data point (at 1.5 hr) onward. The J_{max} value determined from the J_{app2} calculation was approximately 3% too high. However, t_{jmax} shifted in time from the earliest minutes of the experiment to 1.5 hr. In addition, the J_{app2} estimate at time zero was 1.2 (mg /cm^2 hr), substantially above a reasonable, near zero value. The very inaccurate J_{app2} value at time zero was due to a lack of early time data, when the intrinsic flux and receiver concentration were changing most rapidly.

In such circumstances, when there are very few early data points, the more accurate method for estimation of J_{max} and t_{jmax} is the inverse Laplace method of Sclafani et al (1).

The applicability of the J_{app2} approximation to a bilayer membrane was then tested. The bilayer diffusion model generated receiver concentration values for various second layer effective diffusivity (D_{e2}) values. By only altering D_{e2}, the resistance of the first layer remained constant while the resistance of the second layer changed. Thus, the overall resistance of the membrane and the relative resistances of the individual layers were affected.

In Figure 6, the intrinsic flux and the apparent flux J_{app2} are plotted for various effective diffusivities (D_{e2}). The transport properties of the first layer were the same as those used in Figures 1 - 5. For these calculations h_2 = 305 μm and K_2 = 1.0. The D_{e2} value was varied from 3.05×10^{-8} to 1.0 ×

Table II. Intrinsic and Apparent (J_{app1}) Flux Data from Sclafani et al. (1) for Ethanol Diffusing Through Human Skin[a]

Time (hr)	J_{intrin} (mg/cm^2 hr)	J_{app1} (mg/cm^2 hr)	C_{rec} (mg/ml)	J_{app2} (mg/cm^2 hr)
0.00	0.00	0.00	0.00	1.20
1.50	1.42	0.97	1.02	1.51
3.50	1.32	1.26	1.33	1.36
5.50	1.21	1.26	1.33	1.23
7.50	1.12	1.17	1.23	1.11
9.50	1.03	1.09	1.15	1.04
11.50	0.95	1.01	1.07	0.97
13.50	0.87	0.96	1.01	0.90
15.50	0.81	0.84	0.89	0.79
17.50	0.74	0.81	0.85	0.77
19.50	0.68	0.72	0.76	0.67
21.50	0.63	0.65	0.69	0.61
23.50	0.58	0.60	0.63	0.57

[a] C_{rec} values calculated using Equation 3 and J_{app2} values from Equation 4. The maximum intrinsic flux was 1.47 mg/cm^2 hr and occurred within 5–10 min.

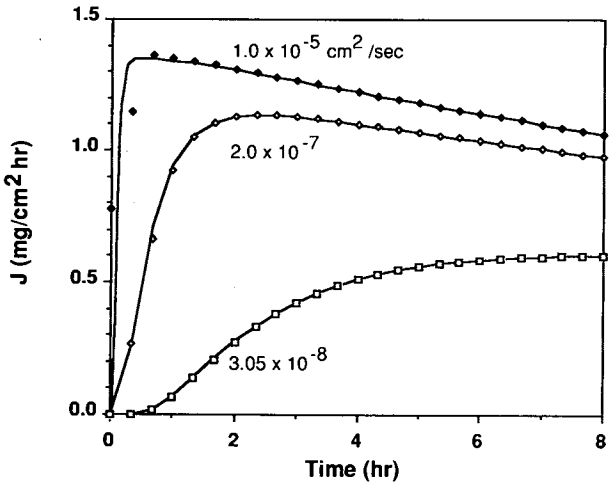

Fig. 6. Effect of D_{e2} on the intrinsic flux and apparent flux J_{app2} for a bilayer membrane. V_{don} = 0.5 ml, V_{rec} = 6 ml, F_{rec} = 4 ml/hr. Transport properties of the first layer same as those given in Figure 2. K_2 = 1.0 and H = 325 μm. D_{e2} values as listed.

10^{-5} (cm^2/sec), thus altering the relative resistance of the first layer from 50% to 99.7%, respectively.

As seen in Figure 6, the J_{app2} values provided excellent approximations to the intrinsic fluxes over the range of D_{e2} values. As the overall membrane resistance increased, the t_{jmax} values also increased. With the constant sampling interval of 20 min shown in Figure 6, there was an effective increase in the number of early time data points with increasing membrane resistance. Therefore the accuracy of the J_{app2} calculation improved. It was clear that the J_{app2} values provided a good estimate of the flux out of the second layer of the skin when >99% of the overall resistance resided in the first layer. When the resistance of one layer becomes significantly greater than the resistance of the other, the bilayer membrane model and the single layer membrane model yield the same result.

CONCLUSIONS

The results confirmed that, in general, the J_{app1} approximation was not an accurate estimate of the intrinsic flux, particularly in the earliest phases of the diffusion experiment prior to the peak in the receiver cell concentration. In addition, the J_{app1} estimate did not produce accurate values of J_{max} or t_{jmax}. The J_{app2} approximation was an accurate estimate of the intrinsic flux over the entire course of the experiment, except at time zero. The J_{max} and t_{jmax} values determined from J_{app2} were also quite accurate. The J_{app2} expression was significantly better because it accounted for accumulation of drug within the receiver compartment, which the J_{app1} expression did not. However, for very slowly permeating drugs, or very small receiver volumes combined with high flow rates, the effect of accumulation would be small and the J_{app1} estimation would become reasonably accurate.

Larger receiver volumes and lower flow rates could be used experimentally to obtain reliable estimates of intrinsic flux, since J_{app2} was essentially independent of V_{rec}, F_{rec} and V_{don}. Therefore, significantly higher drug concentrations would be permissible in the receiver chamber and the accuracy of the concentration measurement may be substantially increased.

In order to properly account for accumulation of drug in the receiver cell, concentration data at the earliest times were required. If early time data were not available, a previously published inverse Laplace method was more accurate than the J_{app2} approach.

ACKNOWLEDGMENTS

We appreciate the support of this work from NICHD-R01-23000.

REFERENCES

1. J. Sclafani, J. Nightingale, P. Liu, and T. Kurihara-Bergstrom. Flow-Through System Effects on *in Vitro* Analysis of Transdermal Systems. *Pharm. Res.* **10**: 1521-1526 (1993).
2. E. R. Cooper. Increased Skin Permeability for Lipophilic Molecules. *J. Pharm. Sci.* 73: 1153-1156 (1984).
3. V. M. Knepp, R. S. Hinz, F. C. Szoka, and R. H. Guy. Controlled Drug Release From a Novel Liposomal Delivery System. I. Investigation of Transdermal Potential. *J. Controlled Release.* 5: 211-221 (1988).
4. T. Kai, V. H. W. Mak, R. O. Potts, and R. H. Guy. Mechanism of Percutaneous Penetration Enhancement: Effect of n-Alkanols on the Permeability Barriers of Hairless Mouse Skin. *J. Controlled Release.* **12**: 103-112 (1990).
5. W. J. Addicks, G. L. Flynn, and N. Weiner. Validation of a Flow-Through Diffusion Cell for Use in Transdermal Research. *Pharm. Res.* **4**: 337-341 (1987).
6. W. Addicks, N. Weiner, G. Flynn, R. Curl, and E. Topp. Topical Drug Delivery from Thin Applications: Theoretical Predictions and Experimental Results. *Pharm. Res.* 7: 1048-1054 (1990).
7. W. G. Reifenrath, B. Lee, D. R. Wilson, and T. S. Spencer. A Comparison of In Vitro Skin-Penetration Cells. *J. Pharm. Sci.* 83: 1229-1233 (1994).
8. R. L. Bronaugh and R. F. Stewart. Methods for In Vitro Percutaneous Absorption Studies IV: the Flow-Through Diffusion Cell. *J. Pharm. Sci.* **74**: 64-67 (1985).
9. S. A. Akhter, S. L. Bennett, I. L. Waller, and B. W. Barry. An Automated Diffusion Apparatus for Studying Skin Penetration. *Inter. J. Pharm.* **21**: 17-26 (1984).
10. M. Goodman and B. W. Barry. Lipid-Protein-Partitioning (LPP) Theory of Skin Enhancer Activity: Finite Dose Technique. *Inter. J. Pharm.* 57: 29-40 (1989).
11. A. C. Williams and B. W. Barry. Terpenes and the Lipid-Protein-Partitioning Theory of Skin Penetration Enhancement. *Pharm. Res.* 8: 17-24 (1991).
12. D. Friend, P. Catz, J. Heller, J. Reid, and R. Baker. Transdermal Delivery of Levonorgestrel I: Alkanols as Permeation Enhancers In Vitro. *J. Controlled Release.* 7: 243-250 (1988).
13. D. R. Friend, P. Catz, J. Heller, and M. Okagaki. Transdermal Delivery of Levonorgestrel. V. Preparation of Devices and Evaluation in Vitro. *Pharm. Res.* **6**: 938-944 (1989).
14. P. Catz and D. R. Friend. Transdermal Delivery of Levonorgestrel. VIII. Effect of Enhancers on Rat Skin, Hairless Mouse Skin, Hairless Guinea Pig Skin, and Human Skin. *Inter. J. Pharm.* 58: 93-102 (1990).
15. M. Akazawa, T. Itoh, K. Masaki, B. T. Nghiem, N. Tsuzuki, R. Konishi, and T. Higuchi. An Automated Method for Continuously Monitoring Diffusion Cells in Skin Penetration Studies. *Inter. J. Pharm.* **50**: 53-60 (1989).
16. K. Knutson, D. J. Harrison, L. K. Pershing, and C. Y. Goates. Transdermal Absorption of Steroids. *J. Controlled Release.* **24**: 95-108 (1993).
17. H. Durrheim, G. L. Flynn, W. I. Higuchi, and C. R. Behl. Permeation of Hairless Mouse skin I: Experimental Methods and

Comparison with Human Epidermal Permeation by Alkanols. *J. Pharm. Sci.* **69**: 781-786 (1980).
18. P. Liu, T. Kurihara-Bergstrom, and W. R. Good. Cotransport of Estradiol and Ethanol Through Human Skin in Vitro: Understanding the Permeant/Enhancer Flux Relationship. *Pharm. Res.* **8**: 938-944 (1991).
19. L. A. Kurtz, R. E. Smith, C. L. Parks, and L. R. Boney. A Comparison of the Method of Lines to Finite Difference Techniques in Solving Time-Dependent Partial Differential Equations. *Computers and Fluids*. **6**: 49-70 (1978).
20. A. C. Hindmarsh. LSODE and LSODI, Two New Initial Value Ordinary Differential Equation Solvers. *ACM-Signum Newsletter*. **15**: 10-11 (1980).
21. H.-K. Choi and J. T. Angello. Mathematical Analysis and Optimization of a Flow-Through Diffusion Cell System. *Pharm. Res.* **11**: 595-599 (1994).